AD-A138 794 FILM COOLING ON A GAS TURBINE BLADE NEAR THE END WALL 1/1
(U) MINNESOTA UNIV MINNEAPOLIS DEPT OF MECHANICAL
ENGINEERING R J GOLDSTEIN ET AL. MAY 83
UNCLASSIFIED AFOSR-TR-84-0109 F49620-83-C-0062 F/G 21/5 NL

END
DATE FILMED
4-84
DTIC

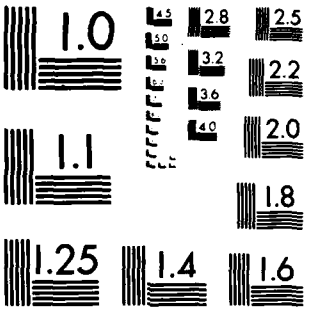

MICROCOPY RESOLUTION TEST CHART
NATIONAL BUREAU OF STANDARDS-1963-A

UNCLASSIFIED

SECURITY CLASSIFICATION OF THIS PAGE (When Data Entered)

(4)

REPORT DOCUMENTATION PAGE		READ INSTRUCTIONS BEFORE COMPLETING FORM
1. REPORT NUMBER AFOSR-TR- 84-0109	2. GOVT ACCESSION NO.	3. RECIPIENT'S CATALOG NUMBER
4. TITLE (and Subtitle) FILM COOLING ON A GAS TURBINE BLADE NEAR THE END WALL		5. TYPE OF REPORT & PERIOD COVERED INTERIM 6. PERFORMING ORG. REPORT NUMBER
7. AUTHOR(s) R J GOLDSTEIN H P CHEN		8. CONTRACT OR GRANT NUMBER(s) F49620-83-C-0062
PERFORMING ORGANIZATION NAME AND ADDRESS UNIVERSITY OF MINNESOTA DEPT OF MECHANICAL ENGINEERING MINNEAPOLIS, MN 55455		10. PROGRAM ELEMENT, PROJECT, TASK AREA & WORK UNIT NUMBERS 61102F 2307/A4
CONTROLLING OFFICE NAME AND ADDRESS AIR FORCE OFFICE OF SCIENTIFIC RESEARCH/NA BOLLING AFB, DC 20332		12. REPORT DATE May 1983 13. NUMBER OF PAGES 8
MONITORING AGENCY NAME & ADDRESS(If different from Controlling Office)		15. SECURITY CLASS. (of this report) Unclassified 15a. DECLASSIFICATION DOWNGRADING SCHEDULE

DISTRIBUTION STATEMENT (of this Report)

pproved for Public Release; Distribution Unlimited.

DISTRIBUTION STATEMENT (of the abstract entered in Block 20, if different from Report)

18 SUPPLEMENTARY NOTES

19 KEY WORDS (Continue on reverse side if necessary and identify by block number)

FLUID MECHANICS
INTERNAL FLOWS
HEAT TRANSFER
FILM COOLING
GAS TURBINE
TURBINE BLADE

20 ABSTRACT (Continue on reverse side if necessary and identify by block number)

The local film cooling effectiveness on cooling a gas turbine blade with a row of discrete cooling jets has been measured using a mass transfer technique. Particular emphasis is placed on phenomena near the end wall of the blade. This region contains a horseshoe vortex system modified by a passage vortex. On the concave (pressure) surface the film cooling performance is not greatly altered by the presence of the end wall. On the convex surface of the blade the film cooling is essentially absent in a triangular region extending from near the region of peak curvature

DD FORM 1 JAN 73 1473 EDITION OF 1 NOV 65 IS OBSOLETE

UNCLASSIFIED

SECURITY CLASSIFICATION OF THIS PAGE (When Data Entered)

on the blade to its trailing edge. This unprotected region closely corresponds to the location of the passage vortex as indicated by flow visualization. The passage vortex sweeps away the injected coolant flow from the surface. Upstream of the unprotected area the injected flow is skewed toward the middle span of the blade. The influence of the end wall extends about one-half cord length up from the end wall in the present experiments.

FILM COOLING ON A GAS TURBINE BLADE NEAR THE END WALL

R. J. Goldstein and H. P. Chen
Mechanical Engineering Department
University of Minnesota

ABSTRACT

The local film cooling effectiveness on a gas turbine blade with a row of discrete cooling jets has been measured using a mass transfer technique. Particular emphasis is placed on phenomena near the end wall of the blade. This region contains a horseshoe vortex system modified by a passage vortex. On the concave (pressure) surface the film cooling performance is not greatly altered by the presence of the end wall. On the convex surface of the blade the film cooling is essentially absent in a triangular region extending from near the region of peak curvature on the blade to its trailing edge. This unprotected region closely corresponds to the location of the passage vortex as indicated by flow visualization. The passage vortex sweeps away the injected coolant flow from the surface. Upstream of the unprotected area the injected flow is skewed toward the middle span of the blade. The influence of the end wall extends about one-half cord length up from the end wall in the present experiments.

NOMENCLATURE

a_1-a_2	attachment line - Figure 5
C_{iw}	concentration of tracer at impermeable wall
C_2	concentration of tracer in injected gas--usually measured in plenum
D	diameter of injection hole
h	heat transfer coefficient
H	distance along blade surface from end wall
M	blowing rate $\rho_2 U_2/\rho_\infty U_\infty$
I	momentum flux ratio $\rho_2 U_2^2/\rho_\infty U_\infty^2$
q	wall heat flow per unit time and area
R	density ratio ρ_2/ρ_∞
S_{S1}	saddle point - Figure 5
S_1-S_2	seperation line - Figure 5
T	temperature
T_{aw}	adiabatic wall tempertaure
Tr	wall recovery temperature
T_w	wall temperature
T_2	temperature of injected flow
U_2	mean velocity in injection hole
U_∞	mainstream velocity at injection hole location
X	distance downstream of downstream edge of injection holes
Z	transverse distance from center of injection hole to sampling hole; measured towards the end wall in present tests
α	angle between the injection hole centerline and local blade surface; 35° in present tests
η_{aw}	local adiabatic film-cooling effectiveness

NOMENCLATURE CON'T.

η_{iw} local impermeable -wall effectiveness

ρ_2 density of injected flow

ρ_∞ density of mainstream

δ_{99} boundary layer thickness; distance from wall where velocity is 99% of free stream velocity

INTRODUCTION

Over the last decade, the average temperature of combustion gas entering the first stage turbine in high performance aircraft gas turbines has increased from 1500K to 1750K; of this 250K increase, improved alloys contributed 65K while improved cooling contributed the rest [1]. In the next decade, the entry temperature in some turbine systems is expected to surpass 1900K, yet alloys generally must stay under 1300K [1]. To prevent high-temperature failure, further improvements in cooling methods such as film cooling, and internal convection and impingement heat transfer are required.

The present work is concerned with film cooling - a process in which a coolant injected along a surface exposed to a high temperature gas flow reduces the temperature of the boundary layer and hence the surface.

In studies of film cooling an adiabatic wall effectiveness is generally defined by:

$$\eta_{aw} = \frac{T_{aw} - T_r}{T_2 - T_r} \qquad (1)$$

and the heat transfer is calculated from:

$$q = h\,(T_w - T_{aw}) \qquad (2)$$

When η_{aw} and h are known, the local heat transfer can be calculated. Studies on full-coverage film cooling and transpiration cooling often use somewhat different definitions of heat transfer coefficient.

Early studies on film cooling on flat walls are reviewed in Ref. [2]. The effectiveness in two-dimensional incompressible film cooling mainly depends on the blowing rate, M, injection slot size and the position downstream of injection. A heat sink model has been successfully used to analyze such a cooling system. For film cooling with injection through discrete holes, the local effectiveness also depends on the transverse position and the relative densities of the injected and mainstream fluids. A heat sink model for three-dimensional film cooling is mainly useful at low blowing rates and when there is not significant interaction among the injected jets. On gas turbine blades with discrete injection, the blade surface curvature and the two end walls make the problem more complex.

The influence of wall curvature on film cooling is most pronounced with injection through discrete holes [3, 4]. Measurments on a linear turbine cascade [4] show the importance of the curvature of the wall surface and the momentum flux of the injected jets relative to that of the mainstream. Thus, at low blowing rates (really, small momentum flux ratio, I), the film cooling effectiveness is better on a convex surface than on a flat plate, which, in turn, has better performance than a concave surface. This relative performance on surfaces of different curvature reverses at large momentum flux ratios. These differences are due to the influence of the pressure gradient normal to the surface and its effect on the curvature of the injected jets which can be distinct from the curvature of the mainstream. The influence of curvature on film cooling performance is considerably reduced with coolant injection through two rows of holes [5].

The present work is an experimental study of the influence of the end wall on film cooling of gas turbine blades using a single row of injection holes. In many gas turbines, the blade span is not large compared to the chord length, and a significant region on the blade is influenced by the end wall. Studies of the velocity field and heat transfer in the end wall region of a blade [6, 7, 8] show the complex flow in this region, which includes a horseshoe vortex system and a passage vortex in the region between two adjacent blades. Those studies are valuable in establishing the nature of the flow regime which helps explain experimental results of heat transfer and film cooling on the blades themselves.

EXPERIMENTAL SYSTEM AND TEST CONDITIONS

The experiments are conducted in a low velocity wind tunnel using a linear cascade of six turbine blades [4]. The inlet and outlet angles of the blade are 45.7° and 27.3°, respectively and the angle of attack of the incoming flow is close to zero. The dimensions of the blade are enlarged several times over normal size with a chord length in the cascade of 16.9 cm. Four of the blades are solid. The two central ones are hollow, and are used to provide film cooling--on facing suction (convex) and pressure (concave) surfaces. The diameter of the injection holes is 2.38 mm; they are inclined at an angle 35° to the surface, and spaced three diameters apart. A mixture of air and helium is used as the injected fluid; the density is kept at approximately 0.96 that of the freestream. Blowing rates, M, of 0.5 on the convex surface and 0.8 and 1.55 on the concave surface are used. These three blowing rates correspond to values of I of, .26, .67, and 2.5, respectively.

The mass/heat transfer analogy is used

to determine the film cooling effectiveness. Instead of measuring an adiabatic temperature, the flow is essentially isothermal and the injected flow contains a tracer gas (helium in the present study). The concentration of the helium tracer gas is measured in samples drawn from near the wall through small (0.58 mm diam) sampling taps. As the concentration of helium in the mainstream is zero, the local impermeable wall effectiveness is the ratio of the helium concentration at the wall to that in the plenum which contains the injected fluid,

$$\eta_{iw} = C_{iw}/C_2 \qquad (3)$$

The gas samples are collected during a run and later analyzed with a gas chromatograph utilizing a thermal conductivity cell detector. The sampling holes are distributed across the span at Z locations 0, 0.5, 1.0, and 1.5 diameters from the center of one of the injection holes, and at various positions downstream.

Figure 1 shows the positions of the holes and the sampling taps. The blade can be moved into or out of the end wall by moving it through a slot in the wall. Note that the four rows of sampling taps used are some distance apart. For a single positioning of the blade relative to the end wall, the measurements are taken for each row of sampling taps. These represent the regions between different injection holes. To get a consistent set of data for results between a given pair of holes (at fixed H/D) four different positionings of the blade must be used.

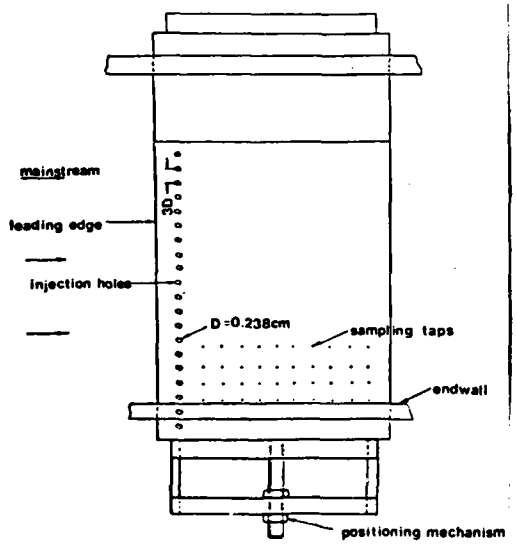

Figure 1a. Test Blade - View of Suction Side

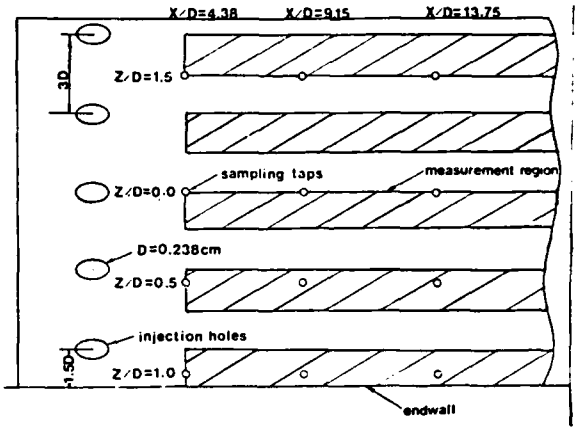

Figure 1b. Detail of Test Blade Showing Measurement Region

The lowest coolant hole was centered 1-1/2 diameters from the end wall. By moving the blade to somewhat more than a dozen different locations into or out of the end wall, a series of measurements can be taken which represent the area immediately below (i.e. towards the end wall) the lowest twelve holes. The shaded areas show the regions over which the effectiveness can be measured. Note that these represent only *one-half of* the surface as the sampling taps were designed for a study in the central span of a blade where the flow is essentially symmetrical around an injection hole. This can be observed in the data (e.g. Figure 6) where curves are drawn through the set of four data points which correspond to the position below each of the holes studied. These holes are positioned such that their centers are, 1-1/2, 4-1/2, 7-1/2, ... and 37-1/2 diameters from the end wall.

As measurements are taken, only over half of the area, there may be a slight error in the average effectiveness at different heights. In the case of essentially symmetric flow around a blade hole, this would not be important. However, in the end wall region, the flow is not symmetric; rather the jet is skewed either down towards the end wall or up towards the center of the span.

The mainflow velocity at the injection location is 19.8 m/s on the convex surface and 4.6 m/s on the concave surface. The flow of the mainstream approaching the blade cascade is approximately 11 m/s; the boundary layer of this flow on the end wall has a thickness of, $\delta_{99} \cong 2$ cm.

FLOW VISUALIZATION

Flow near the end wall of a blade is studied using a mixture of fine carbon powder and oil spread on contact paper attached to the end wall and the blade surfaces.

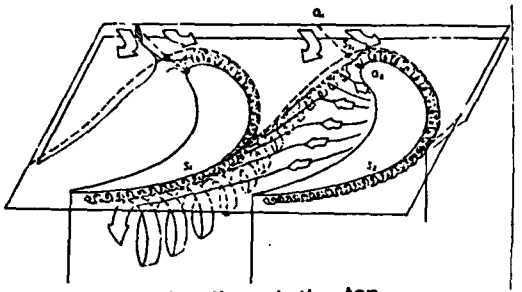

Figure 5. Sketch of the Flow Near Endwall of Gas Turbine Blade

region is at an elevation of 4.3 cm above the end wall. Outside the triangular region, the streamlines near the convex surface are skewed toward the middle span of the blade (cf. Fig. 3). As Fig. 4 indicates, the streamlines by the concave surface are slightly inclined toward the end wall, apparently from the flow that enters into the passage vortex along the end wall. As the distance from the end wall increases, the skew of streamlines on both blade surfaces is reduced. Accurate determination of the flow direction near the blade surface is difficult, as gravity plays a role in the motion of the fluid on the contact paper. However, the general trends are clear in the region close to the passage vortex.

IMPERMEABLE WALL EFFECTIVENESS

Convex Surface

Figure 6 shows the local effectiveness on the convex surface of the blade. Note that the values of Z/D>0 are all measured towards the end wall and as mentioned above, because of the limited number of sampling taps, only one-half of the region between any adjacent pair of injection holes is examined.

From the local measurements at a blowing rate of 0.5 and a density ratio of .96, different regions on the convex blade surface can be specified in terms of the local flow characteristics and film cooling performance. These areas are mapped out in figure 7. Region A is an unprotected region where the film coolant has essentially been stripped from the wall, or displaced by flow from the end wall; the size and shape of this region coincides closely with those of the passage vortex system determined in the visualization tests (cf Figure 3) and described in the section on flow visualization. If the end wall had been film cooled, perhaps some of the coolant might have flowed up into region A. Region B adjacent to this unprotected region is protected by the jets but the flow is skewed due to the presence of the passage vortex beneath region B; this results in a variation of local effectiveness which is not the same as in the two-dimensional flow region (Region D). Thus,

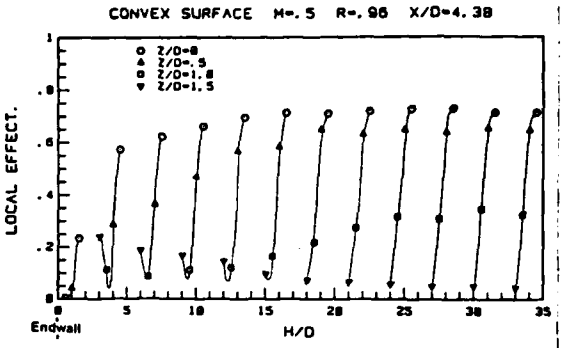

Figure 6a. Local Film Cooling Effectiveness on Convex Surface at M=0.5

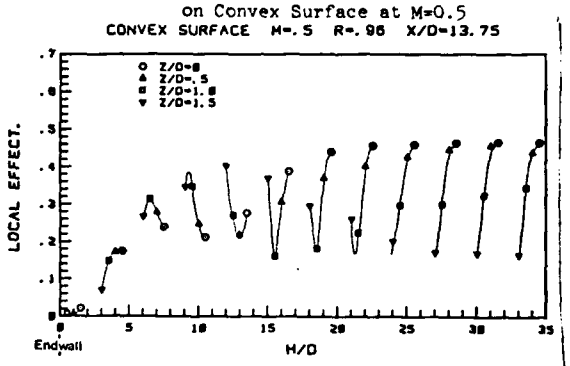

Figure 6b. Local Film Cooling Effectiveness on Convex Surface at M=0.5

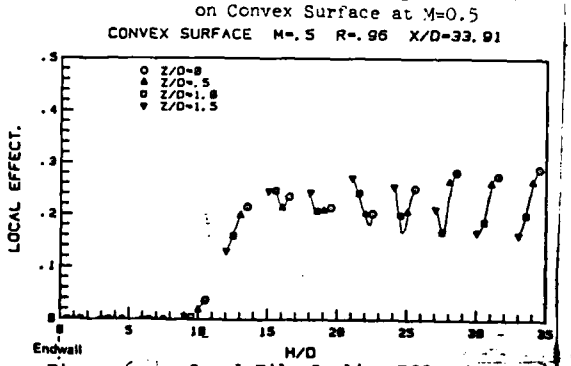

Figure 6c. Local Film Cooling Effectiveness on Convex Surface at M=0.5

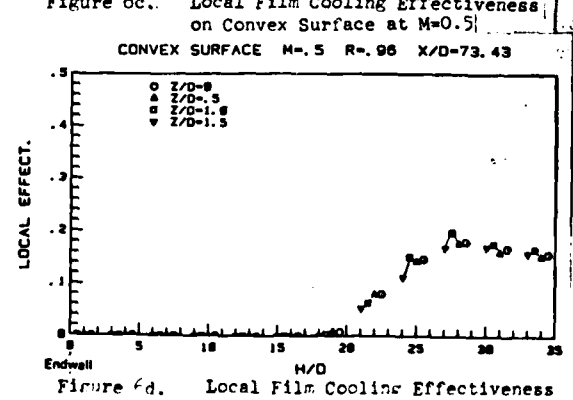

Figure 6d. Local Film Cooling Effectiveness on Convex Surface at M=0.5

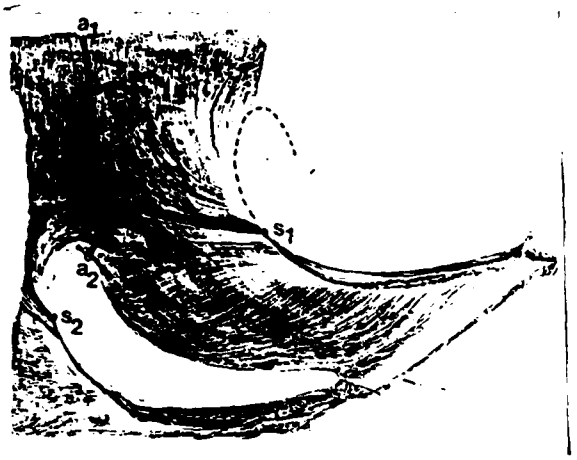

Figure 2. Streamline Tracks on Endwall of Gas Turbine Blade

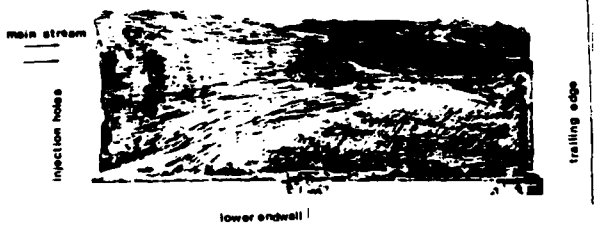

Figure 3. Streamline Tracks on Convex Surface of Gas Turbine Blade

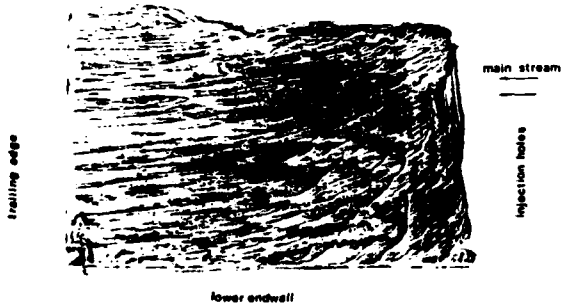

Figure 4. Streamline Tracks on Concave Surface of Gas Turbine Blade

During exposure to the tunnel flow, the streamlines are traced on the paper. Figures 2, 3, and 4 show traces recorded on the end wall, convex surface and concave surface, respectively. These results are in accord with those presented in Ref. [7], with a slight deviation on the concave surface. In the present study, skewing is observed of the flow over the concave surface with streamlines bent down toward the end wall. The flow phenomena can also be inferred from the present measurements of film cooling effectiveness on the concave surface. The lines drawn on Figure 2 are discussed below in the description of Figure 5.

When a circular cylinder is exposed to a crossflow, the mainstream velocity near the front stagnation region decreases and the static pressure rises. In the three-dimensional region near the wall at the base of the cylinder, the velocity in the boundary layer is less than that in the mainstream. The result is a pressure gradient along the cylinder and a velocity component towards the wall which leads to a horseshoe vortex flow. Similarly, in the end wall region of a gas turbine blade, a horseshoe vortex system is formed, but the development of the flow is assymmetric. This is substantially due to the presence of a passage vortex, which, in turn, is due to the difference in pressure across the passage between two blades, with pressure being higher on the concave (pressure) side as compared to the convex (suction) side. Away from the end wall, this pressure difference is balanced by inertia forces as the flow curves around the blades. In the end wall region where the boundary layer is present, the inertia forces are not sufficient to overcome the pressure difference and a flow is established from the pressure side of one blade towards the suction side of the adjacent blade.

The passage vortex is shown in Fig. 5, along with the two legs of the horseshoe vortex formed around the blade (cf. Ref [7]) A separation line, indicated by S1-S2, is present in the boundary layer in front of a blade. The attachment line, a1-a2, extends from the incoming flow to the front stagnation point. It intersects the separation line at the saddle point, S_{S1}. These lines are also drawn on the flow traces in Figure 2. In front of the saddle point, the attachment line divides incoming flow entering the blade passage from that entering the adjacent passage. After the saddle point it divides the passage crossflow moving on to the convex surface of the neighboring blade from the flow moving around the leading edge of the blade onto the convex surface of the same blade. The leg of the horseshoe vortex formed on the pressure side of the blade is moved over towards the suction side of the adjacent blade by the passage vortex, which constantly feeds into the flow causing it to develop into a large vortex. The vortex that is formed initially on the suction side tends to diminish as it flows around the blade because of its opposite sense to that of the passage vortex. It finally becomes a small counter (corner) vortex or can be almost completely dissipated. The exact flow field in the end wall region depends on the position of the saddle point and the strength of the passage vortex which relate to the geometry of the blade cascade and incoming flow conditions, including angle of attack, incoming boundary layer thickness, and Reynolds number.

The passage vortex sweeps across the convex surface of the blade some distance from the stagnation region. The affected region on the blade appears to have a clear boundary and an almost triangular shape--in the present system, the trailing edge of the

where one might expect the maximum effectiveness to occur at a constant transverse position, for example at Z/D=0, in region B it occurs at different values of Z/D for different positions H, from the end wall. Region C, close to the end wall and near the injection holes is not strongly affected by the horseshoe vortex or the passage vortex which has not reached the suction surface here. However, the presence of the boundary layer on the end wall reduces the mainstream flow in the region of these injection holes, giving an equivalent blowing rate or momentum flux ratio greater than that in the two dimensional flow region and, for the injection rate in the present study, a lower effectiveness.

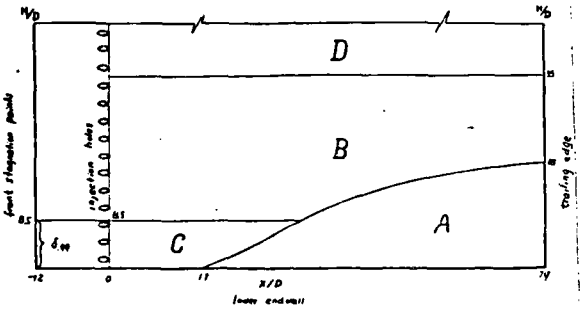

Figure 7. Distribution Range of Local Film Cooling Effectiveness in Endwall Region on Convex Surface of a Blade

The average effectiveness on the convex surface as a function of position from the end wall is shown in Figure 8. These values are obtained by averaging the four points (at different Z/D) determined for each setting of the blade. Recall again, that Z is measured towards the end wall and the average is obtained for only half of the area between each pair of holes. The value of H/D corresponds to the average position, i.e. Z/D=0.75 for each setting. At X/D of 73.4, approximately 93% of the distance along the surface of the blade from the front stagnation line to the trailing edge of the blade, region A (cf. Fig. 7) extends out to H/D of approximately 18. The outline of region A can be inferred from Figure 8. The average effectiveness in region B is not greatly different from that in the two dimensional region.

Concave Surface

On the concave surface of the blade, results are presented for two blowing rates, M=0.8 and M=1.53. For these conditions, values of local effectiveness are plotted on Figure 9 and 11, and values of average effectiveness are shown on Figure 10 and 12.

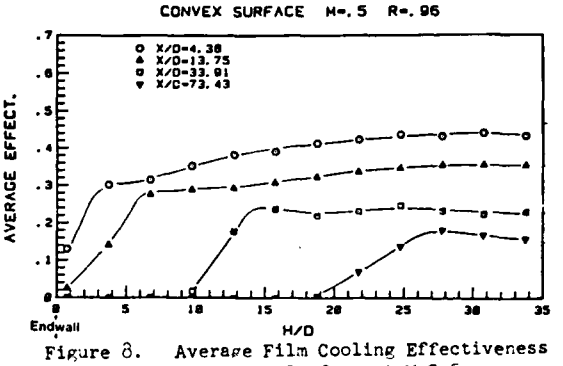

Figure 8. Average Film Cooling Effectiveness on Convex Surface at M=0.5

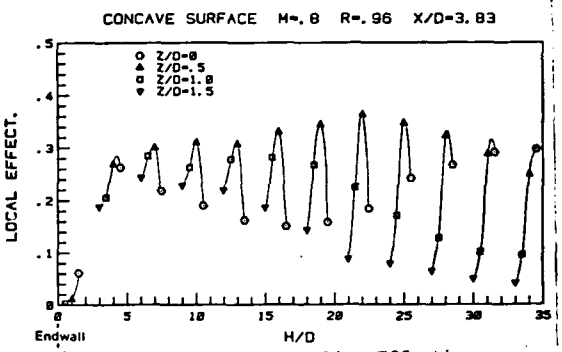

Figure 9a. Local Film Cooling Effectiveness on Concave Surface at M=0.8

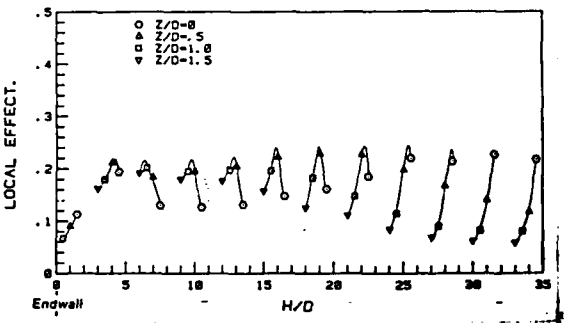

Figure 9b. Local Film Cooling Effectiveness on Concave Surface at M=0.8

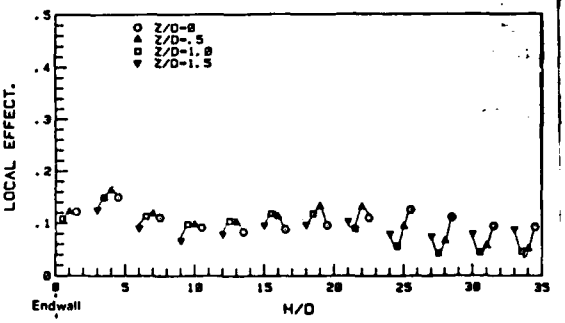

Figure 9c. Local Film Cooling Effectiveness on Concave Surface at M=0.8

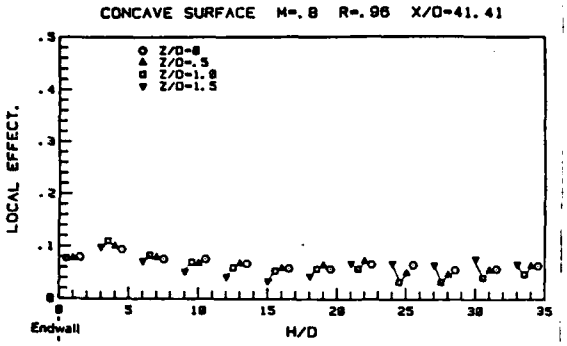

Figure 9d. Local Film Cooling Effectiveness on Concave Surface at M=0.8

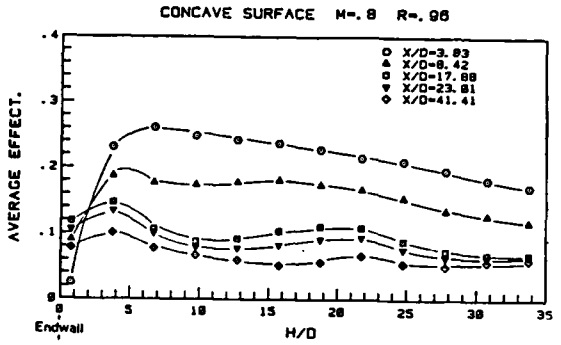

Figure 10. Average Film Cooling Effectiveness on Concave Surface at M=0.8

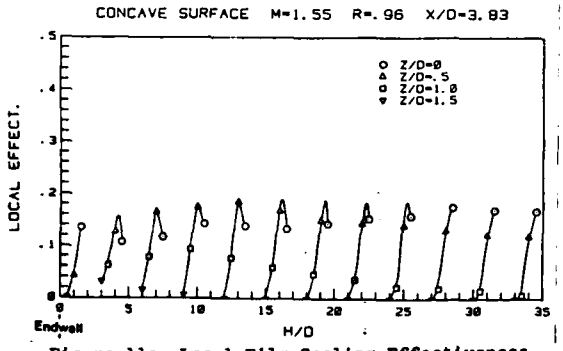

Figure 11a. Local Film Cooling Effectiveness on Concave Surface at M=1.55

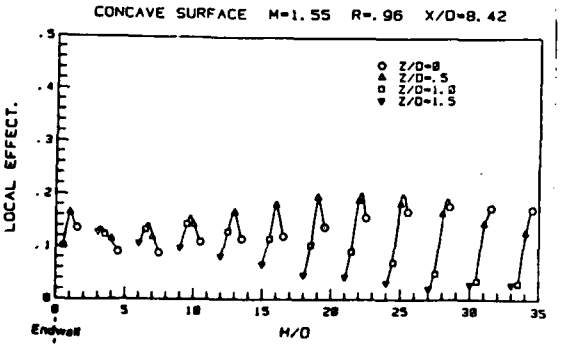

Figure 11b. Local Film Cooling Effectiveness on Concave Surface at M=1.55

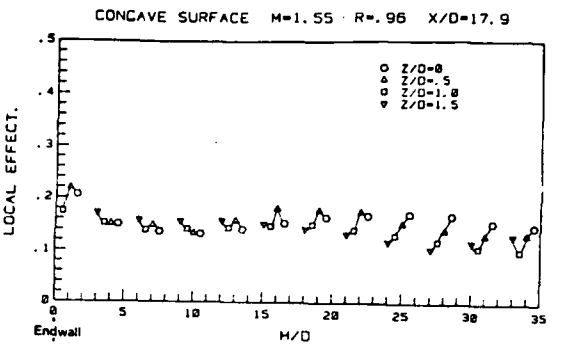

Figure 11c. Local Film Cooling Effectiveness on Concave Surface at M=1.55

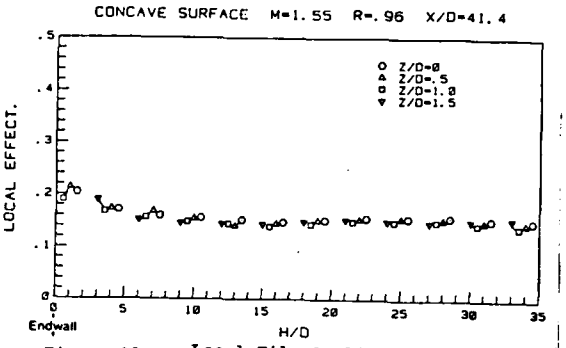

Figure 11d. Local Film Cooling Effectiveness on Concave Surface at M=1.55

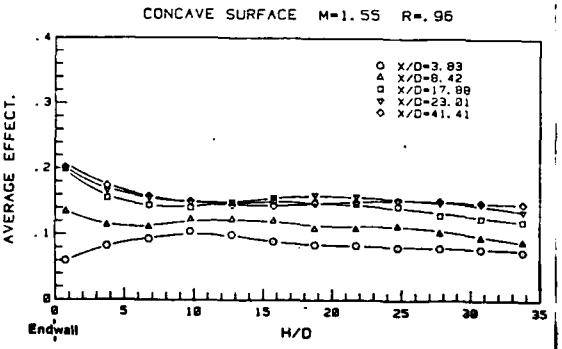

Figure 12. Average Film Cooling Effectiveness on Concave Surface at M=1.55

On the concave surface the film cooling effectiveness is not greatly altered by the presence of the end wall. There is an influence of the flow feeding into the passage vortex moving the injected flow, essentially skewing it towards the end wall, which changes the periodicity or phase of the local effectiveness relative to Z/D. The inclination of the streamlines is slight, compared to that on the convex surface. The difference is average effectiveness, relative to that in the two dimensional region, at small values H/D may be due to the presence of the boundary layer on the end wall and its effect on the local value of M or I, as well as the cross flow due to the fluid

flowing into the passage vortex. In addition, the flow washing down the blade towards the end wall can result in a piling up of the film coolant near the end wall.

CONCLUSIONS

On the convex surface of a gas turbine blade there is a significant region close to the end wall over which the film cooling jets are essentially swept away from the surface by the presence of a passage vortex. This region commences some distance downstream of injection, near the location where the passage vortex reaches the convex surface. Above this region, away from the end wall, the film cooling jets are skewed changing the distribution of local effectiveness, but the average effectiveness is not greatly altered. Film cooling on the concave surface is not significantly affected by the end wall. In some regions it is improved over that in the central portion of the blade span, at least under the present test conditions.

The dimensions over which the influence of the end wall is felt on actual blades will depend on the geometry of the blades and the incoming flow conditions. Further studies are necessary to define the parameters that control the size of the unprotected region along the convex surface.

ACKNOWLEDGEMENT

This study was conducted with support from the U.S. Air Force Office of Scientific Research. P. H. Chen was instrumental in the final preparation of this manuscript.

AFOSR Contract #- F49620-83-C-0062

REFERENCES

1. D. K. Hennecke, "Turbine Blade Cooling in Aeroengines", Von Karman Institute for Fluid dynamics, Lecture Series 1982-02., and personal communication.

2. R. J. Goldstein, "Film Cooling", Advances in Heat Transfer, Vol. 7, Academic Press, New York and London, 1971, pp. 321-379.

3. J. Nicholas and A. LeMeur, "Curvature Effect on a Turbine Blade Cooling Film", ASME paper 74-GT-156, 1974.

4. S. Ito, R. J. Goldstein and E. R. G. Eckert, "Film Cooling of a Gas Turbine Blade", ASME Journal of Engineering for Power, Vol. 100, July 1978, pp. 476-480.

5. R. J. Goldstein, Y. Kornblum, E. R. G. Eckert, "Film Cooling Effectiveness on a Turbine Blade", to be published in Israel Journal of Technology.

6. L. S. Langston, L. M. Nice and R. M. Hooper, "Three-Dimensional Flow within a Turbine Cascade Passage", ASME paper 76-GT-50.

7. L. S. Langston, "Crossflows in a Turbine Cascade Passage", ASME paper 80-GT-5, 1980.

8. R. A. Graziani, M. F. Blair, J. R. Taylor, and R. E. Mayle, "An Experimental Study of Endwall and Airfoil Surface Heat Transfer in a Large Scale Turbine Blade Cascade", ASME Journal of Engineering for Power, Vol. 102, April 1980, PP. 257-267.

ED
84